Improving the use of laser scanning intensity data in complex 3D mapping of the cave environment

Case study of the Gouffre Georges Cave, France

EGU General Assembly 2020

Michaela Nováková[1], Michal Gallay[1], Jozef Šupinský[1], Eric Ferré[2], Patrick Sorriaux[3]

[1] Pavol Jozef Šafárik University in Košice, Institute of Geography, Slovakia
[2] University of Louisiana at Lafayette, School of Geosciences, Lafayette, United States
[3] Association française de karstologie et Spéléo Club du Haut Sabarthez, Tarascon sur Ariège, France

Introduction

Terrestrial laser scanning (TLS) provides a contactless method of acquiring highly detailed and accurate 3D point clouds efficient in mapping the underground forms. Cave surveying with TLS enables exploring features difficult to be reached and studied directly, e.g. speleothems, ceiling channels, structural rock properties alongside with the tectonic features. Besides the 3D coordinates, the intensity of the backscattered laser pulse is recorded. This additional attribute, commonly used for improving point cloud visualization, is influenced by various factors including scanning geometry and properties of the surface material. After elimination of the influencing factors taking into account specifics of the cave environment, the corrected intensity value depends mostly on the spectral surface properties and reveals different lithological layers.

Study area and data acquisition

Gouffre Georges cave is located in the French Pyrenees, near lake Étang de Lers in Ariége department. Part of the cave formed on the contact of marble and lherzolite, ultramafic igneous rock originated in the upper mantle [1]. This contact is significantly visible in the Grande Galerie dome accessible via a closable entrance Tube (1390 m).

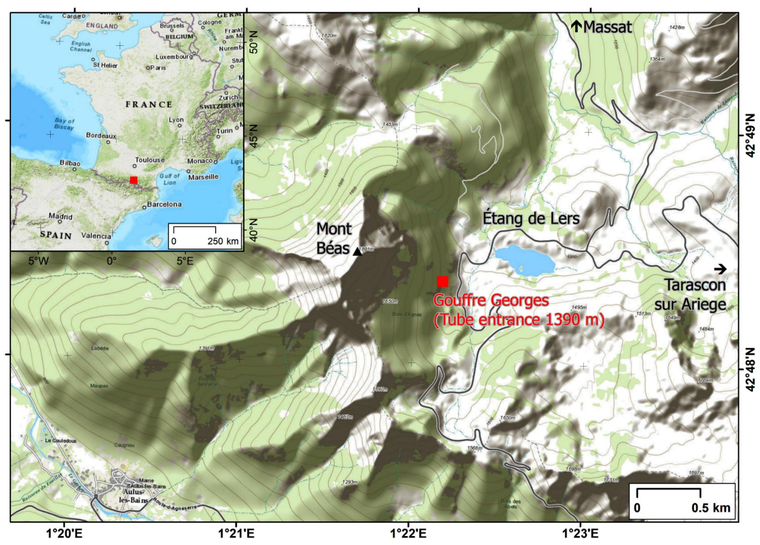

Data acquisition in Salle de la Famine and Grande Galerie domes was realized using TLS Riegl VZ 1000 emitting laser beam in near-infrared wavelength of 1550 nm. Scanning range starting at 0.9 m to 1,400 m allows capturing not only the distant and hardly accessible cave objects but also the exterior. Its robust construction allows scanning in adverse conditions preventing device damaging during transfer and abseiling to lower parts of the cave.

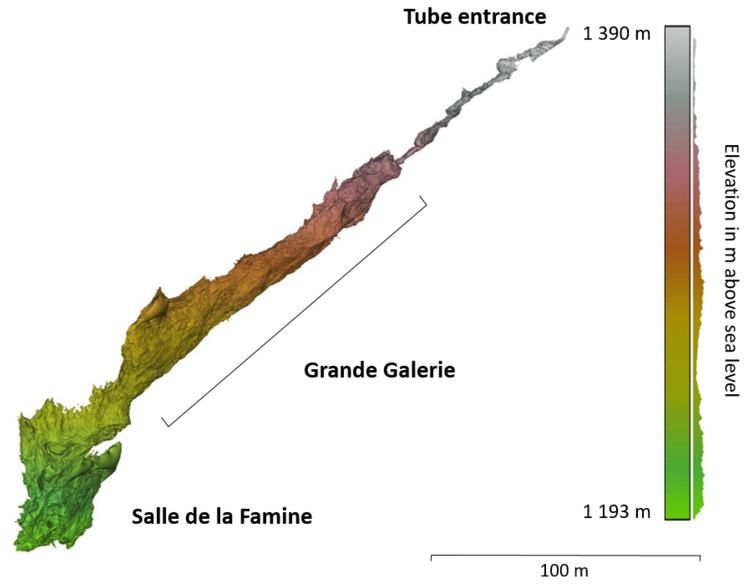

Data processing

The data after collection contained 924,543,719 points, the cave passages represented 47 positions with 655,934,737 points. 26 positions of cave exterior with 268,608,982 points were captured mainly for external registration and information of surface above the cave. Internal registration of scanning positions was processed in RiSCAN PRO software. The resulting internal data registration error was StDev=0.0067 m. Points captured below 2.5 m, declared as minimal scanning range for the device, were removed due to high positional inaccuracy. For obtaining intensity value corresponding with the surface reflectance, only points recorded as single echo of full emitted pulse should remain. Points captured as multiple echoes or points with high deviation were filtered.

Intensity correction

Electromagnetic waves of laser and radar follow the same principles, therefore the radar equation can be used to describe significant parameters affecting the received backscattered power P_r [2]:

$$P_r = \frac{P_t D_r^2}{4\pi R^4 \beta_t^2} \eta_{sys} \eta_{atm} \sigma_{cross}$$

Transmitted pulse power P_t, diameter of the TLS sensor receiver aperture D_r and system transmission factor η_{sys} depend on the sensor and can be considered constant. For target larger than the laser beam with surface corresponding to the perfect diffuse reflector of Lambertian model, the cross-section σ_{cross} can be described as [3]:

$$\sigma_{cross} = \pi \rho_\lambda R^2 \beta_t^2 \cos(\alpha)$$

Where ρ_λ is the surface reflectivity at certain wavelength λ, R is the distance between the TLS and scanned object, β_t is the laser beam width and α is the incidence angle between the surface normal and incident laser beam. After substituting σ_{cross} and simplifying for constants, radar equation can be expressed as [3]:

$$P_r = \rho_\lambda R^{-2} \cos(\alpha) \eta_{atm}$$

The backscattered power P_r is automatically converted into Digital Number [DN] as a scaled integer value for intensity I [4]. Main physical parameters, described as a function of the distance effect $F_1(R)$, incidence angle $F_2(\alpha)$, atmospheric attenuation $F_3(\eta_{atm})$ and surface reflectivity $F_4(\rho_\lambda)$, affect the TLS intensity value as following:

$$I = F_1(R) * F_2(\alpha) * F_3(\eta_{atm}) * F_4(\rho_\lambda)$$

For obtaining the corrected intensity value I_c, depending only on the object surface properties $I_c = F_4(\rho_\lambda)$, other influencing factors should be eliminated. Returned intensity I_{dB} for used TLS device is given in [dB], which can be expressed as [2]:

$$I_{dB} = 10 \log(I)$$

Correction of distance effect

The distance effect does not follow the R^{-2} relation for near distances less than around 15-20 m as a result of brightness reduction and defocusing of the receiver optics [2]. For the used TLS Riegl VZ 1000 the distance effect was derived based on an experiment using reference target scanned for distances starting from 2.5 m, next scanning position at 3 m from the device, and then each position with increment 1 m up to 60 m (target 1-58). Incidence angle was set to 0° to eliminate its influence. The collected intensity data were then fit by a set of polynomial functions for scanning ranges 2.5 - 5 m, 5-15 m, 15-60 m.

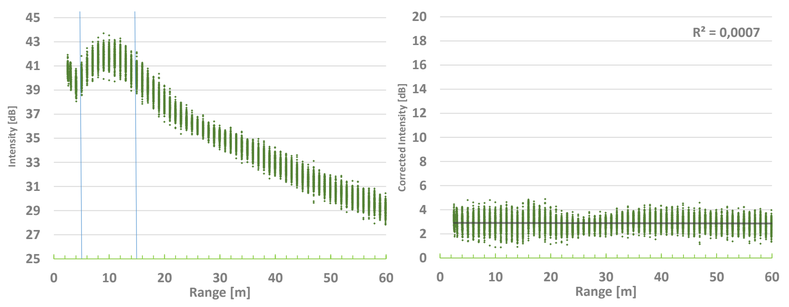

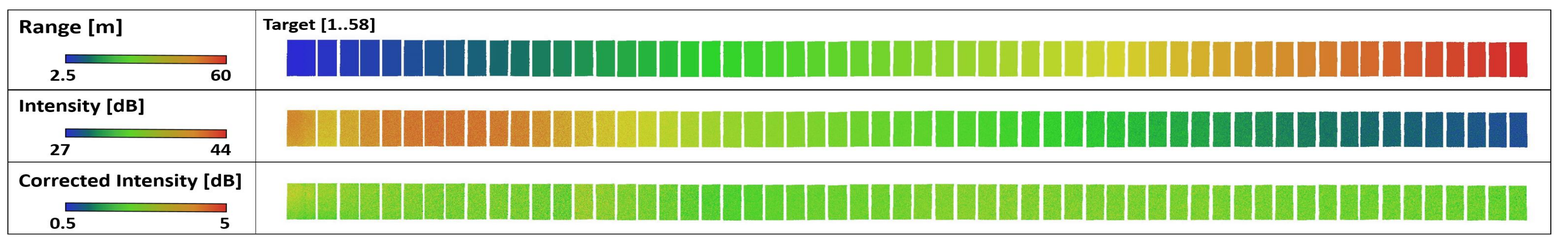

Correction of incidence angle effect

Object with a rough surface, especially the natural rock surfaces, may differ from the Lambertian model of perfect diffuse reflector. To reduce the over-correction for high incidence angle effect of the Lambertian model, the effect of incidence angle α was corrected using the Oren-Nayar physical model of light reflection, describing the surface as a set of facets with different orientations [3].

$$F_2(\alpha) = \cos(\alpha)(A + B \sin(\alpha) \tan(\alpha))$$

$$A = 1 - 0{,}5 \frac{\sigma_{slope}^2}{\sigma_{slope}^2 + 0.33} \qquad B = 0{,}45 \frac{\sigma_{slope}^2}{\sigma_{slope}^2 + 0.09}$$

Parameter σ_{slope} depends only on the surface roughness and can be determined from the pointcloud. Facets were extracted in CloudCompare software with plugin FACETS [5] and the orientation of each facet was interpolated into corresponding points.

Correction of atmospheric attenuation effect

Atmospheric attenuation η_{atm} as is a function of range R and atmospheric attenuation coefficient a and represents the loss of energy caused by scattering and absorption due to atmospheric conditions during scanning [4].

$$\eta_{atm} = 10^{-2Ra/10000}$$

For the cave environment, conditions are rather stable depending on the vicinity of the entrance. High concentration of particles is common in the form of aerosol consisting of pollen, spores, dust and water droplets. Deeper into the cave and farther from the entrance, where vadose seepage or flowing water is present, relative humidity is stable and close to 100% [6]. The attenuation coefficient a was determined based on overlapping data from different scanning positions after elimination of the distance and incidence angle effect and computed as energy attenuation [dB/km] per distance R.

Results

Intensity correction was performed on each of the 47 scans from Gouffre Georges. For results demonstration, the scanning position number 19 from Grande Galerie is presented. Raw intensity data firstly increases with increasing scanning range up to around 12 m and then decreases for longer ranges up to 60 m. After elimination of the influencing factors related to complex cave walls geometry, the resulting corrected intensity values depend mostly on the surface spectral properties and significantly improve the material differentiation, which is beneficial particularly in those areas, where conventional methods are limited due to light conditions and inaccessibility. Derived values reveal different lithological contacts allowing remote lithological mapping and visualizing in 3D. Besides the semi-automatic classification, the recognition, localization and measurement of the features in the point cloud is possible. However, filtration and denoising steps, preceding the delimitation of the values for each rock type is necessary, since the conditions of the surface, water content and active karst processes are still valid.

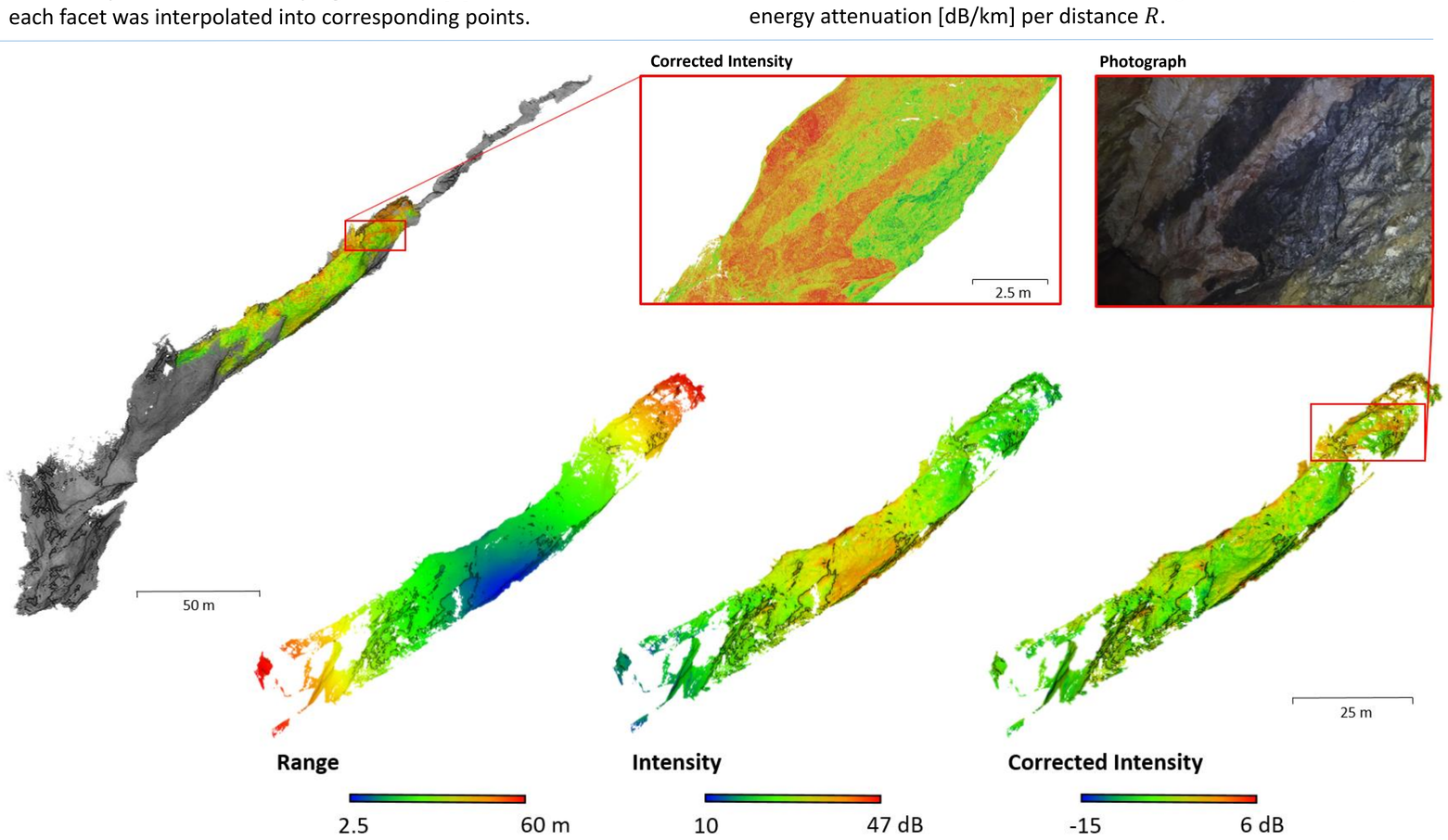

Acknowledgements:

This research was funded by the grant of the Ministry of Education, Science, Research and Sport of the Slovak Republic within the project VEGA 1/0798/20: Synergistic use of multisource remote sensing data in Earth system research.

References

[1] Sorriaux, P. et al. (2019). Expédition spéléo-scientifique au gouffre Georges: Relevé 3D de la Grande galerie. *Spelunca*, *5*.
[2] Xu, T., et al., (2017) Terrestrial Laser Scanning Intensity Correction by Piecewise Fitting and Overlap-Driven Adjustment. *Remote Sensing*, 9(11), 1090.
[3] Carrea, D. et al. (2016) Correction of terrestrial LiDAR intensity channel using Oren–Nayar reflectance model: An application to lithological differentiation. *ISPRS Journal of Photogrammetry and Remote Sensing*, 113, 17-29.
[4] Höfle, B., Pfeifer, N. (2007). Correction of laser scanning intensity data: Data and model-driven approaches. *ISPRS journal of photogrammetry and remote sensing*, 62(6), 415-433.
[5] Dewez, T. et al. (2016). Facets: A cloudcompare plugin to extract geological planes from unstructured 3d point clouds. *ISPRS - International Archives of the Photogrammetry, Remote Sensing and Spatial Information Sciences*. XLI-B5. 799-804.
[6] James, J. M. (2013). Atmospheric processes in caves. *Shroder, J.(Editorin Chief), Frumkin, A.(Ed.), Treatise on Geomorphology. Academic Press, San Diego, CA*, *6*, 304-318.